

# Sensitivity of Quantum Motion to Perturbation in Triangle Map

Wen-ge Wang

*Department of Modern Physics, University of Science and Technology of China, Hefei 230026, China*

*Department of Physics, National University of Singapore, 117542, Singapore*

(Dated: March 24, 2008)

We study quantum Loschmidt echo, or fidelity, in the triangle map whose classical counterpart has linear instability and weak chaos. Numerically, three regimes of fidelity decay have been found with respect to the perturbation strength  $\epsilon$ . In the regime of weak perturbation, the fidelity decays as  $\exp(-c\epsilon^2 t^\gamma)$  with  $\gamma \simeq 1.7$ . In the regime of strong perturbation, the fidelity is approximately a function of  $\epsilon t^{2.5}$ , which is predicted for the classical fidelity [G. Casati, *et al*, Phys. Rev. Lett. **94**, 114101 (2005)], and decays slower than power-law decay for long times. In an intermediate regime, the fidelity has approximately an exponential decay  $\exp(-c'\epsilon t)$ .

PACS numbers: 05.45.Mt, 05.45.Ac, 05.45.Pq

## I. INTRODUCTION

The stability of quantum motion in dynamical systems, measured by quantum Loschmidt echo [1], has attracted much attention in recent years. The echo is the overlap of the evolution of the same initial state under two Hamiltonians with slight difference in the classical limit,  $M(t) = |m(t)|^2$ , where

$$m(t) = \langle \Psi_0 | \exp(iHt/\hbar) \exp(-iH_0 t/\hbar) | \Psi_0 \rangle \quad (1)$$

is the fidelity amplitude. Here  $H_0$  and  $H$  are the unperturbed and perturbed Hamiltonians, respectively,  $H = H_0 + \epsilon H_1$ , with  $\epsilon$  a small quantity and  $H_1$  a perturbation. This quantity  $M(t)$  is called fidelity in the field of quantum information [2].

Fidelity decay in quantum systems whose classical counterparts have strong chaos with exponential instability, has been studied well [3, 4, 5, 6, 7, 8, 9, 10, 11, 12, 13, 14, 15, 16, 17]. Related to the perturbation strength, previous investigations show the existence of at least three regimes of fidelity decay: (i) In the perturbative regime in which the typical transition matrix element is smaller than the mean level spacing, the fidelity has a Gaussian decay. (ii) Above the perturbative regime, the fidelity has an exponential decay with a rate proportional to  $\epsilon^2$ , usually called the Fermi-golden-rule (FGR) decay of fidelity. (iii) Above the FGR regime is the Lyapunov regime in which  $M(t)$  has usually an approximate exponential decay with a perturbation-independent rate.

Fidelity decay in regular systems with quasiperiodic motion in the classical limit has also attracted much attention [9, 14, 17, 18, 19, 20, 21, 22, 23, 24, 25]. For single initial Gaussian wavepacket, the fidelity has been found to have initial Gaussian decay followed by power law decay [9, 21, 25].

Meanwhile, there exists a class of system which lies between the two classes of system mentioned above, namely, between chaotic systems with exponential instability and regular systems with quasiperiodic motion. One example of this class of system is the triangle map proposed by Casati and Prosen [26]. The map has linear instability with vanishing Lyapunov exponent, but can be ergodic

and mixing with power-law decay of correlations. The classical Loschmidt echo in the triangle map has been studied recently and found behaving differently from that in systems with exponential instability and in systems with quasiperiodic motion [27]. This suggests that the decaying behavior of fidelity in the quantum triangle map may be different from that in the other two classes of system as well. In this paper, we present numerical results which confirm this expectation.

Specifically, like in systems possessing strong chaos, in the triangle map three regimes of fidelity decay are found with respect to the perturbation strength: weak, intermediate and strong. However, in each of the three regimes, the decaying law(s) for the fidelity in the triangle map has been found different from that in systems possessing strong chaos. In section II, we recall properties of the classical triangle map and discuss its quantization. Section III is devoted to numerical investigations for the laws of fidelity decay in the three regimes of perturbation strength. Conclusions are given in section IV.

## II. TRIANGLE MAP

On the torus  $(r, p) \in T^2 = [-\pi, \pi) \times [-\pi, \pi)$ , the triangle map is

$$\begin{aligned} p_{n+1} &= p_n + \alpha \operatorname{sgn}(r_n) + \beta, & (\text{mod } 2\pi) \\ r_{n+1} &= r_n + p_{n+1}, & (\text{mod } 2\pi) \end{aligned} \quad (2)$$

where  $\operatorname{sgn}(r) = \pm 1$  is the sign of  $r$  for  $r \neq 0$  and  $\operatorname{sgn}(r) = 0$  for  $r = 0$  [26]. Rich behaviors have been found in the map: For rational  $\alpha/\pi$  and  $\beta/\pi$ , the system is pseudointegrable. With the choice of  $\alpha = 0$  and irrational  $\beta/\pi$ , it is ergodic but not mixing. Interestingly, for incommensurate irrational values of  $\alpha/\pi$  and  $\beta/\pi$ , the dynamics is ergodic and mixing. In our numerical calculations, we take  $\alpha = \pi^2$  and  $\beta = (\sqrt{5} - 1)\pi/2$ , for which  $(\beta/\alpha)$  is an irrational number, the golden mean divided by  $\pi$ , and the map is ergodic and mixing.

The triangle map (2) can be associated with the Hamil-

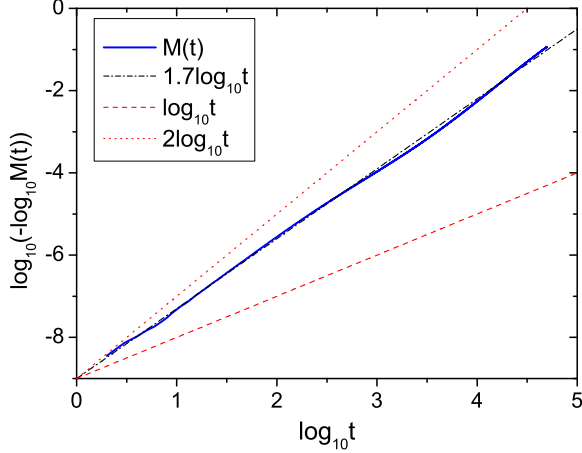


FIG. 1: (color online). Averaged fidelity at weak perturbation,  $\sigma = 10^{-4}$  (solid curve), with average taken over 50 initial point sources chosen randomly,  $N = 2^{12} = 4096$ . The dashed-dotted straight line has a slope 1.7, showing that  $\log_{10} \overline{M}(t)$  is approximately a function of  $t^{1.7}$ . For comparison, we also show two straight lines (dashed and dotted) with slopes 1 and 2, respectively.

tonian

$$H = \frac{1}{2}\tilde{p}^2 + V(r) \sum_{n=-\infty}^{\infty} \delta(t - nT), \quad (3)$$

where  $V(r) = -\tilde{\alpha}|r| - \tilde{\beta}r$  and  $T$  is the period of kicking. It is easy to verify that the dynamics produced by this Hamiltonian gives the map (2) with the replacement  $p = T\tilde{p}$ ,  $\alpha = T\tilde{\alpha}$ , and  $\beta = T\tilde{\beta}$ .

The classical map can be quantized by the method of quantization on torus [28, 29, 30, 31]. Schrödinger evolution under the Hamiltonian in Eq. (3) for one period of time is given by the Floquet operator

$$U = \exp \left[ -\frac{i}{2}(\hat{p})^2 T \right] \exp[-iV(\hat{r})], \quad (4)$$

where we set  $\hbar = 1$  in Schrödinger equation. In this quantization scheme, an effective Planck constant  $\hbar_{\text{eff}} = T$  is introduced. It has the following relation to the dimension  $N$  of the Hilbert space,

$$N\hbar_{\text{eff}} = 4\pi^2, \quad (5)$$

hence,  $\hbar_{\text{eff}} = 2\pi/N$ . In what follows, for brevity, we will omit the subscript eff of  $\hbar_{\text{eff}}$ . Eigenstates of  $\hat{r}$  and  $\hat{p}$  are discretized,  $\hat{r}|j\rangle = j\hbar|j\rangle$  and  $\hat{p}|k\rangle = k\hbar|k\rangle$ , with  $j, k = -N/2, -N/2 + 1, \dots, 0, 1, \dots, (N/2) - 1$ . Then, making use of the above discussed relations among  $\tilde{p}, p, T, \tilde{\alpha}, \alpha, \tilde{\beta}, \beta$ , in particular,  $T = \hbar$ , the Floquet operator in Eq. (4) can be written as

$$U = \exp \left[ -\frac{i}{2\hbar}(\hat{p})^2 \right] \exp \left[ \frac{i}{\hbar}(\alpha|\hat{r}| + \beta\hat{r}) \right]. \quad (6)$$

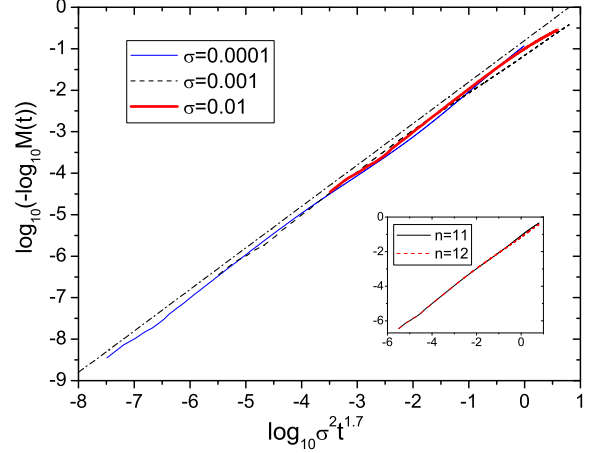


FIG. 2: (color online). Averaged fidelity at three weak perturbation strengths,  $\sigma = 10^{-4}$  (thin solid curve),  $10^{-3}$  (dashed curve), and  $10^{-2}$  (thick solid curve), with average taken over 50 initial point sources chosen randomly,  $N = 2^{12} = 4096$ . The dashed-dotted straight line represents  $M_1(t)$  in Eq. (8) with  $\gamma = 1.7$  and  $c$  as an adjusting parameter. Inset: Fidelity of  $\sigma = 10^{-3}$  and  $N = 2^n$ ; the two curves are almost indistinguishable.

In numerical computation, the time evolution  $|\psi(t)\rangle = U^t|\psi_0\rangle$  is calculated by the fast Fourier transform (FFT) method.

The fidelity in Eq. (1) involves two slightly different Hamiltonians, unperturbed and perturbed. In this paper, for an unperturbed system with parameters  $\alpha$  and  $\beta$ , the perturbed system is given by

$$\alpha \rightarrow \alpha + \epsilon \quad \beta \rightarrow \beta. \quad (7)$$

Without the loss of generality, we assume  $\epsilon \geq 0$ . The parameter  $\sigma = (\epsilon/\hbar)$  can be used to characterize the strength of quantum perturbation.

### III. THREE REGIMES OF FIDELITY DECAY

#### A. Weak perturbation regime

Let us first discuss weak perturbation. As mentioned in the introduction, in systems with strong chaos in the classical limit, the fidelity has a Gaussian decay under sufficiently weak perturbation. The Gaussian decay is derived by making use of the first order perturbation theory for eigensolutions of  $H$  and  $H_0$  and the random matrix theory for  $\Delta E_n \equiv E_n - E_n^0$ , where  $E_n$  and  $E_n^0$  are eigenenergies of  $H$  and  $H_0$ , respectively. Numerical results in Ref. [32] show agreement of the spectral statistics in the triangle map with the prediction of random matrix theory, hence, at first sight, Gaussian decay might be

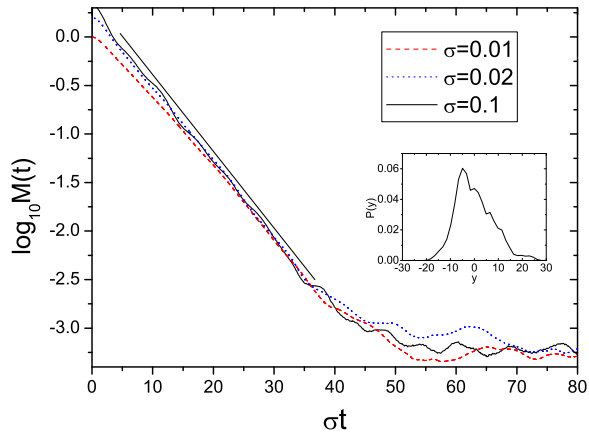


FIG. 3: (color online). Variation of the averaged fidelity with  $\sigma t$  for  $\sigma = 0.01, 0.02$  and  $0.1$ , with average taken over 100 initial point sources chosen randomly,  $N = 4096$ . The solid straight line is drawn for a comparison with linear dependence on  $\sigma t$ . For  $\sigma = 0.02$  and  $0.1$ ,  $\log_{10} \overline{M}(t)$  is approximately a linear function of  $\sigma t$ , before it becomes close to the saturation value. Inset: The distribution  $P(y)$  for the action difference  $\Delta S$  at  $t = 40$ , where  $y = (\Delta S - \langle \Delta S \rangle)/\epsilon$  and  $\langle \Delta S \rangle$  is the average value of  $\Delta S$ . It is calculated by taking randomly  $10^7$  initial points in the phase space.  $P(y)$  does not have a Gaussian shape.

expected for the fidelity decay in the weak perturbation regime of the triangle map.

However, our numerical results show a non-Gaussian decay of fidelity for small perturbation. An example is given in Fig. 1 for  $\sigma = 10^{-4}$ . To obtain relatively smooth curves for fidelity, average has been taken over 50 initial point sources (eigenstates of  $\hat{r}$ ) chosen randomly. This figure, plotted with  $\log_{10}(-\log_{10} \overline{M}(t))$  versus  $\log_{10} t$ , shows clearly that  $\log_{10} \overline{M}(t)$  is approximately proportional to  $t^{1.7}$  (the dashed-dotted straight line), while is far from the Gaussian case of  $t^2$  and the exponential case of  $t$  represented by the dotted and dashed lines, respectively.

Furthermore, we found that the averaged fidelity  $\overline{M}(t)$  can be fitted well by

$$M_1(t) = \exp(-c\sigma^2 t^\gamma) \quad (8)$$

with  $\gamma \simeq 1.7$  and  $c$  as a fitting parameter. In Fig. 2, we show fidelity decay for three different values of  $\sigma$ . With the horizontal axis scaling with  $\log_{10} \sigma^2 t^{1.7}$ , the three curves corresponding to the three values of  $\sigma$  are hardly distinguishable in their overlapping regions (except for long times). Note that, to show clearly the dashed-dotted straight line which represents  $M_1(t)$  in Eq. (8), we have deliberately adjusted a little the best-fitting value of  $c$  such that the dashed-dotted line is a little above the curves of the fidelity.

In the inset of Fig. 2, we show curves of fidelity for the

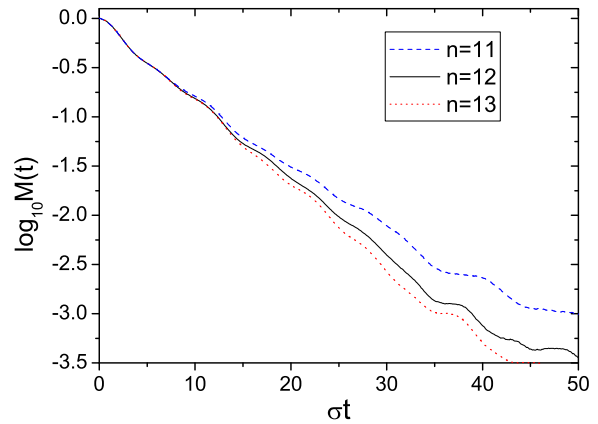


FIG. 4: (color online). Fidelity decay for  $\sigma = 0.1$  and  $N = 2^n$ , averaged over 100 initial point sources.

same  $\sigma$  but different values of  $\epsilon$  and  $N$ . The two curves are very close, supporting the assumption that  $\epsilon$  and  $N$  appear in the form of the single variable  $\sigma$  as written on the right hand side of Eq. (8). This dependence of  $\overline{M}(t)$  on the variable  $\sigma$  for sufficiently small  $\sigma$  can be understood in a first-order perturbation treatment of fidelity, as shown in the following arguments.

Let us consider a Hilbert space with sufficiently large dimension  $N$  and make use of arguments similar to those used in Ref. [8] for deriving the Gaussian decay, but without assuming the applicability of the random matrix theory. It follows that, for times not very long, the averaged fidelity (averaged over initial states) is mainly determined by  $\langle \exp(-i\Delta\omega_n t) \rangle$ , where  $\Delta\omega_n = \omega_n - \omega_n^0$  and  $\langle \dots \rangle$  indicates average over the quasi-spectrum. Here  $\omega_n^0$  is an eigen-frequency of the Floquet operator  $U$  in Eq. (6) and  $\omega_n$  is the corresponding eigen-frequency of  $(Ue^{i\sigma|r|})$ . For large  $N$ ,  $\langle \exp(-i\Delta\omega_n t) \rangle$  can be calculated by making use of the distribution of  $\Delta\omega_n$ . Since the two Floquet operators  $U$  and  $(Ue^{i\sigma|r|})$  differ by  $e^{i\sigma|r|}$ , the distribution of  $\Delta\omega_n$  is approximately a function of  $\sigma$ . Then,  $M(t)$  is approximately a function  $\sigma$ .

Finally, we give some remarks on the value of  $\gamma$ . When  $\Delta\omega_n$  has a Gaussian distribution,  $\overline{M}(t)$  has a Gaussian decay with  $\gamma = 2$ , as in the case of systems possessing strong chaos. In the triangle map, the non-Gaussian decay of fidelity discussed above implies that  $\Delta\omega_n$  does not have a Gaussian distribution. Other types of distribution may predict values of  $\gamma$  different from 2, in particular, a Lévy distribution would give  $\gamma < 2$  in agreement with our numerical result. We also remark that the results here are not in conflict with numerical results of Ref. [32], in which only the statistics of  $\omega_n$  (not that of  $\Delta\omega_n$ ) is found in agreement with the prediction of random matrix theory.

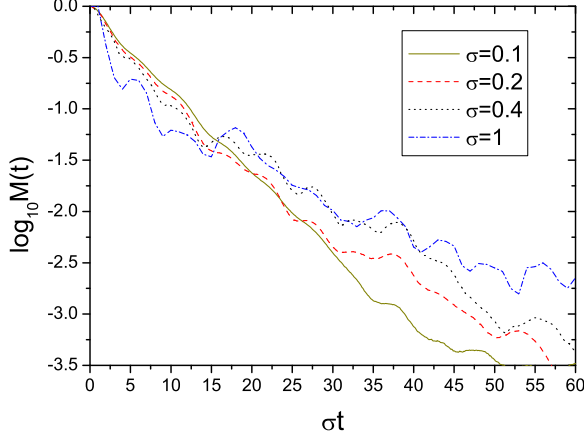


FIG. 5: (color online). Averaged fidelity of  $\sigma$  from 0.1 to 1, with average taken over 1000 randomly chosen initial pointer sources,  $N = 2^{14} = 16384$ . For  $\sigma = 0.2$  and above, the averaged fidelity obeys a decaying law which is different from that in Eq. (9), in particular, it is not a function of  $(\sigma t)$ .

### B. Intermediate perturbation strength

With increasing perturbation strength, exponential decay of  $\overline{M}(t)$  appears (see Fig. 3). For  $\sigma$  from 0.02 to 0.1, after some initial times and before approaching its saturation value, the fidelity decays as

$$M_2(t) = \exp(-a\sigma t), \quad (9)$$

with  $a$  as a fitting parameter. Numerically, we found that  $a \approx 0.08$ . The decay rate is proportional to  $(\sigma t)$ , unlike in the FGR decay found in systems with strong chaos,

$$M_{\text{FGR}}(t) \sim \exp(-2\sigma^2 K_E t), \quad (10)$$

where  $K_E$  is the classical action diffusion constant [8]. The curves of  $\sigma = 0.02$  and  $0.1$  in Fig. 3 are quite close, while that of  $\sigma = 0.01$  has some deviation from the two. This implies that the  $\exp(-a\sigma t)$  behavior of  $\overline{M}(t)$  appears between  $\sigma = 0.01$  and  $0.02$ . Note that vertical shifts have been made for the two curves of  $\sigma = 0.02$  and  $0.1$  in Fig. 3 for better comparison.

The origin of the non-FGR decay of fidelity in this regime of perturbation strength, may come from weak chaos. In fact, in another system which also possesses weak chaos in the classical limit, namely, the sawtooth map in some parameter regime, linear dependence of the decaying rate on  $\sigma$  has also been observed in the intermediate perturbation regime [13, 15, 33]. In this regime of perturbation strength, the semiclassical theory predicts that, in the first order classical perturbation theory, the averaged fidelity is given by [13]

$$\overline{M}(t) \simeq \left| \int d\Delta S e^{i\Delta S/\hbar} P(\Delta S) \right|^2, \quad (11)$$

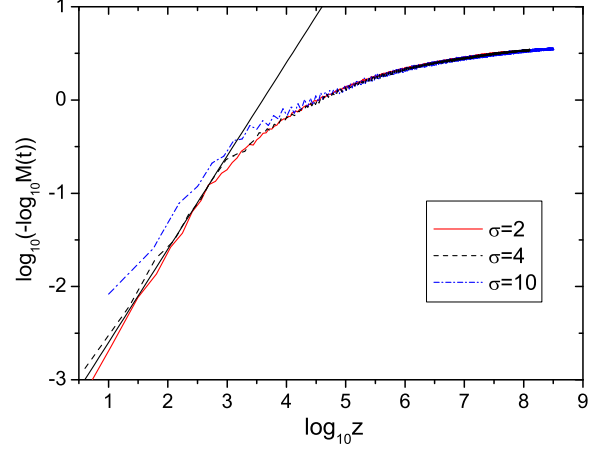


FIG. 6: (color online). Averaged fidelity at strong perturbation, with average taken over 1000 randomly chosen initial Gaussian wavepackets,  $N = 2^{17} = 131072$ .  $z = \epsilon t^{2.5}/\hbar$  with  $\hbar$  fixed in this figure. The solid line represents a curve  $\exp(-c\epsilon t^{2.5})$ , where the fitting parameter  $c$  is determined from comparison with the two curves of  $\sigma = 2$  and  $4$  in the small- $z$  region.

where  $\Delta S(\mathbf{p}_0, \mathbf{r}_0; t) = \epsilon \int_0^t dt' H_1[\mathbf{r}(t')]$  is the action difference of two the classical trajectories starting at the same point  $(\mathbf{p}_0, \mathbf{r}_0)$  in the two systems, with  $H_1$  evaluated along one of the two trajectories, and  $P(\Delta S)$  is the distribution of  $\Delta S(\mathbf{p}_0, \mathbf{r}_0; t)$ . In systems possessing strong chaos,  $P(\Delta S)$  may have a Gaussian form, which implies the FGR decay for the fidelity. In the triangle map,  $P(\Delta S)$  is not a Gaussian distribution as shown in the inset of Fig. 3, hence, the fidelity does not have the FGR decay with a rate proportional to  $\sigma^2$ .

It is difficult to find an analytical expression for  $P(\Delta S)$ , hence, we can not derive Eq. (9) analytically. However, a qualitative understanding of the  $(\sigma t)$ -dependence of  $\overline{M}(t)$  can be gained, as shown in the following arguments. Equation (11) shows that the time-dependence of fidelity decay comes mainly from the dependence of  $P(\Delta S)$  on time. In the case of strong chaos,  $\Delta S$  behaves like a random walk, hence,  $P(\Delta S)$  has a Gaussian form with a width increasing as  $\sqrt{t}$  [8]. Since  $\Delta S \propto \epsilon$ , the width of  $P(\Delta S)$  is a function of  $(\epsilon\sqrt{t})$ ; then, Eq. (11) gives the FGR decay of  $\overline{M}(t)$  which depends on  $(\sigma^2 t)$ . In the case of the triangle map, due to the linear instability of the map, it may happen that the width of  $P(\Delta S)$  increase linearly with  $t$  in some situations when  $t$  is not very long. This implies that the width of  $P(\Delta S)$  may be a function of the variable  $(\epsilon t)$ . Then, it is possible for  $\overline{M}(t)$  to be approximately a function of  $(\sigma t)$ .

Equation (11) predicts that, up to the first order classical perturbation theory, the dependence of  $\overline{M}(t)$  on  $\epsilon$  and  $\hbar$  takes the single variable  $\sigma = \epsilon/\hbar$ . Numerically we found that this is approximately correct, as shown in

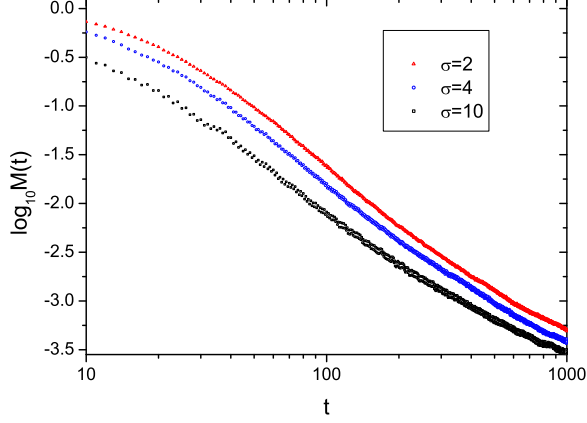


FIG. 7: (color online). Averaged Fidelity for strong perturbation, from top to bottom,  $\sigma = 2, 4$  and  $10$ . The average is taken over 1000 initial Gaussian wavepackets chosen randomly and over time from  $t - 2$  to  $t + 2$ .  $N = 2^{17}$ . The time axis is plotted in the logarithm scale. It shows that the long time decay of fidelity is slower than power law decay.

Fig. 4. Specifically, for fixed  $\sigma = 0.1$ ,  $\overline{M}(t)$  of  $N = 2^{11}$  and of  $N = 2^{12}$  separate at about  $t = 15$ . Indeed, for long times  $t$ , higher order contributions in the classical perturbation theory may need consideration and  $\overline{M}(t)$  may depend on  $\epsilon$  and  $\hbar$  in a different way. For larger  $N$ , hence smaller  $\hbar$ , the agreement becomes better, e.g.,  $\overline{M}(t)$  of  $N = 2^{12}$  is closer to  $N = 2^{13}$  than to  $N = 2^{11}$ .

When  $\sigma$  goes beyond  $0.1$ , the exponential decay of  $\overline{M}(t)$  expressed in Eq. (9) disappears, in particular, the dependence of  $\overline{M}(t)$  on  $\sigma$  and  $t$  does not take the form of  $(\sigma t)$  (see Fig. 5). Meanwhile fluctuations of  $\overline{M}(t)$  becomes larger and larger with increasing  $\sigma$  for initial point states. For example, Fig. 5 shows that  $\overline{M}(t)$  of  $\sigma = 1$  has considerable fluctuations even after averaging over 1000 initial point sources. Taking initial Gaussian wavepackets, the fluctuations can be much suppressed.

### C. Strong perturbation regime

The triangle map has vanishing Lyapunov exponent, hence, its fidelity may not have the perturbation-independent decay which has been observed at strong perturbation in systems possessing exponential instability in the classical limit [3, 7, 12, 16]. To understand fidelity decay in the triangle map, it is helpful to recall results about the classical fidelity given in [27]. In the classical triangle map, the classical fidelity decays as  $M_{cl}(t) \sim \exp(-c\epsilon t^{2.5})$  for initial times when  $M_{cl}(t)$  remains close to one, and has an exponential decay  $\exp(-c'\epsilon^{2/5}t)$  for longer times. The interesting feature is that the classical fidelity depends on the same scaling variable  $\tau \equiv \epsilon t^{2.5}$  in different time regions.

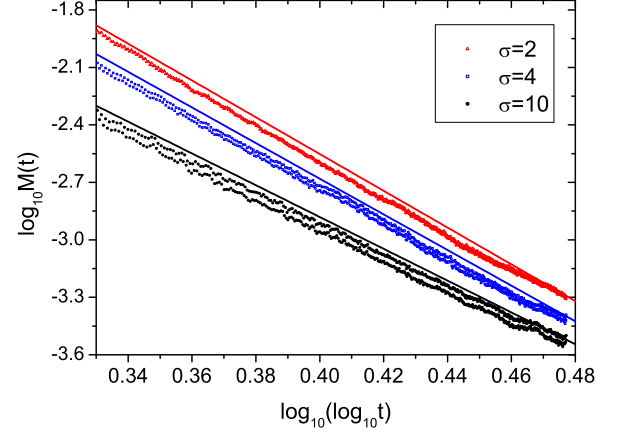


FIG. 8: (color online). The same as in Fig. 7, with a different scale for the horizontal axis and for the time interval  $140 < t < 1000$ . For  $\sigma = 4$  and  $10$ ,  $\log_{10} \overline{M}(t)$  form two lines for each  $\sigma$ . The three solid lines represent  $\log_{10} M_3(t)$  given by Eq. (12), with  $b = 9.6, 9.3$ , and  $8.3$  from top to bottom.

In the weak and intermediate perturbation regimes discussed in the previous sections, the dependence of fidelity on  $\epsilon$  and  $t$  does not take the form of the single variable  $\tau$ . This is not strange, because the classical limit is achieved in the limit  $\hbar \rightarrow 0$ , which implies  $\sigma \rightarrow \infty$  for whatever small but fixed  $\epsilon$ . Therefore, it is the strong perturbation regime in which the decaying behavior of fidelity may have some relevance to the classical fidelity. Numerical results presented below indeed support this expectation.

Figure 6 shows variation of the averaged fidelity with  $\log_{10} \epsilon t^{2.5}$ , with average taken over 1000 initial Gaussian wavepackets chosen randomly. The initial decay of the fidelity of  $\sigma = 2$  and  $4$  are quite close to the classical prediction  $\exp(-c\epsilon t^{2.5})$ . For longer times, the fidelity of  $\sigma$  from  $2$  to  $10$  (with  $\hbar$  fixed) is approximately a function of  $\tau$ , the scaling variable predicted in the classical case, but, the decaying behavior of fidelity is not the same as that of the classical fidelity, i.e., not an exponential decay. We found that the dependence of  $\overline{M}(t)$  on  $\hbar$  does not take the form of  $\tau/\hbar$ , i.e.,  $\overline{M}(t)$  is not a function of the single variable  $(\tau/\hbar)$ .

For long times, the fidelity has large fluctuations even after averaging over 1000 initial Gaussian wavepackets. The fluctuations can be much suppressed, when a further average is taken for time  $t$ . Specifically, for each time  $t$ , we take average over  $\overline{M}(t')$  for  $t'$  from  $t - 2$  to  $t + 2$ . The results are given in Fig. 7, which shows that the long time decay of fidelity is slower than power law decay. To study the decaying behavior of the slower-than-power-law decay, we compare it with the function

$$M_3(t) = a(\log_{10} t)^{-b}, \quad (12)$$

with  $a$  and  $b$  as fitting parameters. In the time interval  $140 < t < 1000$ , the averaged fidelity can be fitted by this

function, as shown in Fig. 8, where we plot  $\log_{10} M(t)$  versus  $\log_{10}(\log_{10} t)$ . Further research work is needed to find analytical explanations for this slower-than-power-law decay of fidelity.

#### IV. CONCLUSIONS AND DISCUSSIONS

We present numerical results on fidelity decay in the triangle map with linear instability. Three regimes of fidelity decay has been found with respect to the perturbation strength: weak, intermediate and strong. At weak perturbation, the fidelity decays like  $\exp(-c\sigma^2 t^{1.7})$ . In the intermediate regime, the fidelity has an exponential decay which is approximately  $\exp(-c'\sigma t)$ . In the regime of strong perturbation, the fidelity is approximately a function of  $\epsilon t^{2.5}$  and decays slower than power law decay

for long times.

These results show that the fidelity in the triangle map obeys decaying laws which are different from those in systems with strong chaos or with regular motion. The difference is closely related to the weak-chaos feature of the classical triangle map. In which way and to what extent does weak chaos influence the fidelity decay? This is still an open question. Indeed, common features of fidelity decay in systems with weak chaos, as well as their explanations, should be an interesting topic for future research work. In particular, one may note that stretch exponential decay of fidelity has also been observed for wave packets which initially reside in the border between chaotic and regular regions in mixed-type systems [34].

**ACKNOWLEDGMENTS.** The author is very grateful to G. Casati and T. Prosen for valuable discussions and suggestions. This work is partially supported by Natural Science Foundation of China Grant No. 10775123 and the start-up funding of USTC.

- 
- [1] A. Peres, Phys. Rev. A **30**, 1610 (1984).
  - [2] M.A. Nielsen and I.L. Chuang, *Quantum Computation and Quantum Information* (Cambridge University Press, Cambridge, 2000).
  - [3] R.A. Jalabert and H.M. Pastawski, Phys. Rev. Lett. **86**, 2490 (2001);
  - [4] Ph. Jacquod, P.G. Silvestrov, and C.W.J. Beenakker, Phys. Rev. E **64**, 055203(R) (2001).
  - [5] F.M. Cucchietti, C.H. Lewenkopf, E.R. Mucciolo, H.M. Pastawski, and R.O. Vallejos, Phys. Rev. E **65**, 046209 (2002).
  - [6] Ph. Jacquod, I. Adagideli, and C.W.J. Beenakker, Phys. Rev. Lett. **89**, 154103 (2002).
  - [7] G. Benenti and G. Casati, Phys. Rev. E **65**, 066205(2002);
  - [8] N. R. Cerruti and S. Tomsovic, Phys. Rev. Lett. **88**, 054103 (2002); J. Phys. A **36**, 3451 (2003).
  - [9] T. Prosen and M. Žnidarič, J. Phys. A **35**, 1455 (2002).
  - [10] W. Wang and B. Li, Phys. Rev. E **66**, 056208 (2002);
  - [11] J. Vaníček and E.J. Heller, Phys. Rev. E **68**, 056208 (2003).
  - [12] P.G. Silvestrov, J. Tworzydło, and C.W.J. Beenakker, Phys. Rev. E **67**, 025204(R) (2003).
  - [13] W. Wang, G. Casati, and B. Li, Phys. Rev. E **69**, 025201(R) (2004).
  - [14] J. Vaníček, Phys. Rev. E **70**, 055201(R) (2004); **73**, 046204 (2006); e-print quant-ph/0410205.
  - [15] Wen-ge Wang and Baowen Li, Phys. Rev. E **71**, 066203 (2005).
  - [16] Wen-ge Wang, G. Casati, B. Li, and T. Prosen, Phys. Rev. E **71**, 037202 (2005).
  - [17] T. Gorin, T. Prosen, T.H. Seligman, and M. Žnidarič, Phys. Rep. **435**, 33 (2006) (quant-ph/0607050).
  - [18] T. Prosen and M. Žnidarič, New J. Phys. **5**, 109 (2003).
  - [19] Ph. Jacquod, I. Adagideli, and C.W.J. Beenakker, Europhys. Lett. **61**, 729 (2003).
  - [20] R. Sankaranarayanan and A. Lakshminarayan, Phys. Rev. E **68**, 036216, 2003.
  - [21] Y.S. Weinstein and C.S. Hellberg, Phys. Rev. E **71**, 016209 (2005).
  - [22] M. Combescure, J. Phys. A **38**, 2635, 2005; M. Combescure, J. Mat. Phys. **47**, 032102, 2006; M. Combescure and D. Robert, quant-ph/0510151.
  - [23] F. Haug, M. Bienert, W. P. Schleich, T. H. Seligman, and M. G. Raizen, Phys. Rev. A **71**, 043803, 2005.
  - [24] S. Wimberger and A. Buchleitner, J. Phys. B **39**, L145, 2006.
  - [25] Wen-ge Wang, G. Casati, and Baowen Li, Phys. Rev. E **75**, 016201 (2007).
  - [26] G. Casati and T. Prosen, Phys. Rev. Lett. **83**, 4729 (1999); *ibid.* **85**, 4261 (2000).
  - [27] G. Casati, T. Prosen, J. Lan, and B. Li, Phys. Rev. Lett. **94**, 114101 (2005).
  - [28] J.H. Hannay and M.V. Berry, Physica D **1**, 267 (1980).
  - [29] J. Ford, G. Mantica, and G.H. Ristow, Physica D **50**, 493 (1991).
  - [30] J. Wilkie and P. Brumer, Phys. Rev. E **49**, 1968 (1994).
  - [31] F. Haake, *Quantum Signatures of Chaos*, 2nd ed. (Springer-Verlag, Berlin, 2001).
  - [32] M. D. Esposti, S. O'Keefe, and B. Winn, Nonlinearity **18**, 1073 (2005).
  - [33] A similar behavior of fidelity decay in a billiard is discussed in D.A. Wisniacki, E.G. Vergini, H.M. Pastawski, and F.M. Cucchietti, Phys. Rev. E **65**, 055206(R) (2002).
  - [34] Y.S. Weinstein, S. Lloyd, and C. Tsallis, Phys. Rev. Lett. **89**, 214101 (2002).